

Optical Code-Division-Multiplexed Systems Based on Spectral Encoding of Noncoherent Sources

M. Kavehrad, *Fellow, IEEE*, and D. Zaccarin

Abstract—In this paper, we present a new category of optical CDMA systems which work based on spectral encoding. In such systems, that we will refer to as Frequency-Encoded CDMA (FE-CDMA) systems, the coding is done in the frequency domain while in the usual CDMA systems the code multiplies the modulation signal in the time domain. We present a new type of FE-CDMA system, based on encoding noncoherent broadband sources. We discuss the advantages of our system compared to other optical CDMA systems and present its performance. We show that very efficient, low-cost, CDMA systems can be obtained with an aggregate throughput of many gigabits per second. Also, for this system, the spreading gain of CDMA is independent of the modulation bandwidth. Hence, the system can accommodate variable bit rates, naturally.

I. INTRODUCTION

IN MOST REPORTS in the literature, CDMA systems design is based on encoding the information signal in the time domain by a pseudorandom sequence. Efficient systems for use in Local Area Network (LAN) environments can be obtained. However, no matter how the system is designed, it will always suffer from a basic limitation. As the number of simultaneous active users is increased, the code length has to be increased in order to maintain the same performance. To do so, without sacrificing the bit rate, one is constrained to use shorter and shorter pulses. When coherent, the required optical sources are likely to be mode-locked lasers producing transform limited pulses, rendering the system expensive and possibly not competitive when compared with those using other access schemes. If an incoherent CDMA system is considered, it might be difficult, at some point, to find lasers for which the coherence time is much shorter than the chip period, a necessary condition for these systems to behave as expected. We should also note that as the pulses used become very short, the chip duration becomes incompatible with the bandwidth of the photodetector, and that optical nonlinear elements, such as AND gates have to be used as in TDMA systems, increasing the cost and the complexity of the system.

It is therefore necessary to find other types of optical CDMA systems, for which increasing the multiple access capacity, i.e. the code length, will not necessarily mean using shorter

pulses or lower bit rates. One possibility is to use different "dimensions" for the code and for the information. In [1], Weiner *et al.*, proposed coding mode-locked pulses in the frequency domain. The information is transmitted using ASK in the time domain. However, the coding in the frequency domain will affect the pulse in the time domain, placing more constraints on the bit rate. Moreover, short pulses are still required and mode-locked lasers have to be used, making the system expensive.

Inspired by their design, we propose an original solution based on encoding in the frequency domain noncoherent optical sources such as edge-emitting LED's (EE-LED) or Super luminescent diodes (SLD). Our system has the advantage of being simple, inexpensive and has a spreading gain totally independent of the bit rate. Part of the following work has been published in [2] and [3]. In the next section, we first present how in practice encoding optical sources can be done in the frequency domain. The encoder is a well-known double-grating apparatus and is common to both our system and the system developed in [1]. In Section III, we focus on FE-CDMA systems that employ noncoherent sources. In Section IV, we present some examples of codes that are suitable for this application. In Section V, we describe the transceiver design. In Section VI, we look at some practical issues in implementation and applications of such a system. In Section VII, we evaluate the performance of our proposed method. In Section VIII, we examine the possibility of using this technique for ATM switching. In Section IX, we discuss our results, and in Section X, we conclude the paper.

II. FREQUENCY ENCODING OF OPTICAL SOURCES

A well-known frequency-encoder for optical sources is shown in Fig. 1. It consists of a pair of diffraction gratings placed at the focal planes of a unit magnification, confocal lens pair. This apparatus has been used with high-efficiency by many research teams for temporal shaping of short pulses, for example see [4]–[5]. The first grating spatially decomposes the spectral components present in the incoming optical signal with a certain resolution. A spatially patterned mask is inserted midway between the lenses at the point where the optical spectral components experience maximal spatial separation. After the mask, the spectral components are re-assembled by the second lens and second grating into a single optical beam. The mask can modify the frequency components in phase and/or in amplitude, depending on the coherence property of the incident optical source. The number of frequency bands that can be resolved by the encoder will dictate the code length,

Manuscript received November 5, 1994; revised December 5, 1994 This work was supported in part by the Telecommunications Research Institute of Ontario (TRIO), Photonics Networks and Systems Thrust and NSERC (Canada.).

M. Kavehrad is with Department of Electrical Engineering, University of Ottawa, Ottawa, Ontario K1N6N5 Canada.

D. Zaccarin is with Bell Northern Research Ltd., Ottawa, Ontario K1Y4H7 Canada.

IEEE Log Number 9409174.

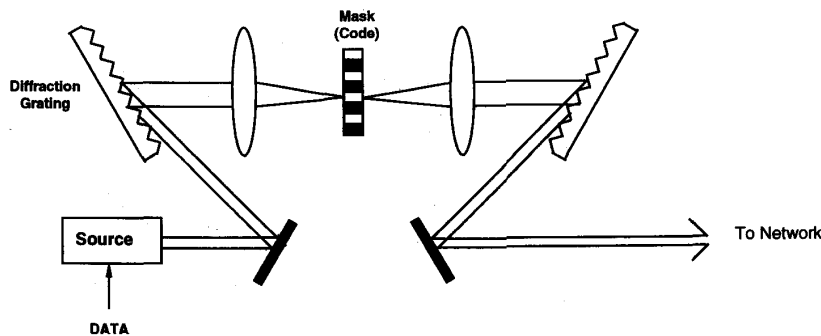


Fig. 1. Frequency encoder for optical sources.

and therefore the number of subscribers in the system. It can be shown [4] that this number is given approximately by

$$N \approx 0.5 \frac{\delta\lambda}{\lambda} \frac{\pi w}{d \cdot \cos(\theta_r)} \quad (1)$$

where λ is the center wavelength of the optical source, $\delta\lambda$ is the spectral width being encoded, w is the input beam radius, d is the grating period and θ_r is the diffracted angle of the central wavelength. For $\delta\lambda = 50$ nm, $\lambda = 1.55$ μm , $w = 3$ mm, $1/d = 1200$ lines/mm grating and $\theta_r = 68^\circ$ (for Littrow configuration), we compute $N \approx 490$ subscribers. Such a spectral width is easily obtained when using noncoherent optical sources such as LED's or superluminescent diode lasers. When using coherent optical sources, it requires a pulse duration of approximately 0.1 ps (100 fs), at that wavelength.

III. FE-CDMA SYSTEMS WITH TEMPORALLY INCOHERENT SOURCES

Since FE-CDMA systems are based on encoding the spectrum of optical sources, natural alternatives to mode-locked lasers are noncoherent sources such as multimode lasers or LED's. For these sources, the large frequency bandwidth is caused by photons being produced with different energy, and is independent of the modulating signal. It is then clear that filtering the spectrum of these sources will not affect the temporal shape of the modulating signal¹. Therefore, the multiple-access capacity cannot be based on the differences of intensity levels between the coded and the uncoded waves. New coding strategies have to be found.

Polychromatic spatially coherent or noncoherent sources have found many applications in the past in different areas such as spectrography, holography [7], optical processing [8] and image transmission [9]–[10]. In transform applications, spatial incoherence allows to avoid coherent noise while the large spectrum is divided into many "wavelength channels" to achieve parallel capacity. Much effort is still being spent by the researchers to achieve achromatic transforms using broadband sources.

In communications applications however, broadband sources such as LED's were until recently, considered as being

¹In fact the signal in the time domain will be only slightly modified [6].

undesirable, laser diodes being the right choice. Mainly three reasons explain this: 1) Lasers couple more light into SMF, 2) they allow a wide variety of modulation types such as DPSK or FSK and 3) they can be modulated at higher bit rates. A number of recent experiments however have demonstrated that light-emitting diodes can be used instead of diode lasers to satisfy many short to medium distance single-mode or multimode system requirements. When compared with diode lasers, LED's offer the advantage of higher reliability, reduced temperature sensitivity, less complicated drive circuit requirements, immunity to optical feedback, and lower cost due to high yields in packaging technology. The cost factor is very important in bringing the optical fiber with transmission capacity of up to 600 Mbt/s to customers in the Subscriber Loop applications [11]. To answer this, extensive research efforts are made to develop "new" types of LED's such as Edge-Emitting LED's (EE-LED) and Superluminescent Diodes (SLD). These LED's are very strong competitors to diode lasers since they can couple high power levels into SMF. As examples, SLD's with average output power of -5 dBm at 1480 nm have been reported [12]. EE-LED's coupling -6 dBm into SMF are available. Such high coupling power is made possible by the fact that the output emission profile is a narrow beam, very similar to that of the lasers. Their modulation bandwidth is also very large compared to Surface-Emitting LED (SE-LED). The amplified spontaneous emission noise (ASE) emitted by erbium-doped fiber amplifiers, usually called broadband Superluminescent Fiber Source [13], is also a good candidate for FE-CDMA systems. Recent experiments show that the ASE can be used as a broadband (more than 30 nm) source with a total output power of 5 mW (+7 dBm). The spectral density of the source has less than 5 dB variation over the 30 nm bandwidth. The coherence length is 210 μm . Recent experiments with EE-LED over 10 km and 20 km of SMF have been conducted at bit rates of 1.2 Gbt/s and 600 Mbt/s [11]. The FWHM of these devices is from 50 nm to ≈ 120 nm so that for CDMA applications, the bandwidth to be encoded is also very large.

All these factors make us believe that EE-LED and SLD could play an important role in future LAN applications. In the next section, we show how LED's could outperform laser diodes in LAN applications using CDMA. This is ac-

complished by using the dimensionality of wavelength. Since the system configuration depends on the codes used, we first describe suitable codes for amplitude coding of LED's.

IV. CODES FOR INCOHERENT FE-CDMA SYSTEMS

Since LED's are temporally incoherent sources, they can not in general retain phase information and the weighting function $W(f)$ used to code the spectrum is constrained to be a unipolar real function. Since the masks used are passive devices we must have $W(f) \leq 1$, and it is immediately apparent that some power loss will occur. Note that, although we consider complete asynchronism between the users, only the periodic correlation parameters are of interest, since the frequency slots of the different users will always be aligned.

Let $(\mathbf{X}) = (x_0, x_1, \dots, x_{N-1})$ and $(\mathbf{Y}) = (y_0, y_1, \dots, y_{N-1})$ be two $(0, 1)$ sequences. The periodic crosscorrelation is

$$\Theta_{\mathbf{X}\mathbf{Y}}(k) = \sum_{i=0}^{N-1} x_i y_{i+k}. \quad (2)$$

Define the complement of sequence (\mathbf{X}) by $(\bar{\mathbf{X}})$ whose elements are obtained from (\mathbf{X}) by $\bar{x}_i = 1 - x_i$. The periodic crosscorrelation sequence between $(\bar{\mathbf{X}})$ and (\mathbf{Y}) is similarly

$$\Theta_{\bar{\mathbf{X}}\mathbf{Y}}(k) = \sum_{i=0}^{N-1} \bar{x}_i y_{i+k}. \quad (3)$$

We look for sequences for which

$$\Theta_{\mathbf{X}\mathbf{Y}}(k) = \Theta_{\bar{\mathbf{X}}\mathbf{Y}}(k) \quad (4)$$

A receiver that computes $\theta_{\mathbf{X}\mathbf{Y}}(k) - \theta_{\bar{\mathbf{X}}\mathbf{Y}}(k)$ will reject the interference coming from user having sequence (\mathbf{Y}) . We first list some sequences that achieve this, and then explain how $\theta_{\mathbf{X}\mathbf{Y}}(k) - \theta_{\bar{\mathbf{X}}\mathbf{Y}}(k)$ can be computed optically.

A. M -Sequences

A unipolar M -sequence of length N is obtained from the bipolar version by replacing each binary 1 by a 0 and each -1 by a 1. Consider the sequence (\mathbf{Y}) as being $(T^k \mathbf{X}) = (\mathbf{X})^k$ where T is the operator that shifts vectors cyclically to the left by one place, that is $(TX) = (x_1, x_2, \dots, x_{N-1}, x_0)$. In that case

$$\Theta_{\mathbf{X}\mathbf{Y}}(k) = \sum_{i=0}^{N-1} x_i x_{i+k} \quad (5)$$

which results in $\theta_{\mathbf{X}\mathbf{Y}}(0) = \frac{N+1}{2}$ for $k = 0$ and to $\theta_{\mathbf{X}\mathbf{Y}}(k) = \frac{N+1}{4}$ for $k = 1$ to $N-1$. The sum $i+k$ is taken modulo N . These results come from the shift-and-add property of M -sequences which says that the modulo-2 sum of an M -sequence and any cycle phase shift of the same M -sequence is another phase of the same sequence. In other words, half the 1's in $(\mathbf{X})^k$ coincide with the 1's of (\mathbf{X}) while the other half coincide with the 0's, where $(\mathbf{X})^k$ is the k cycle shift of

(\mathbf{X}) . A receiver that computes

$$\begin{aligned} Z &= \Theta_{\mathbf{X}\mathbf{Y}}(k) - \Theta_{\bar{\mathbf{X}}\mathbf{Y}}(k) = \sum_{i=0}^{N-1} x_i x_{i+k} - \sum_{i=0}^{N-1} (1-x_i) x_{i+k}, \\ &= 2\Theta_{\mathbf{X}\mathbf{Y}}(k) - \Theta_{\mathbf{X}\mathbf{Y}}(0) \\ &= 2 \times (N+1)/4 - (N+1)/2 \\ &= 0 \end{aligned} \quad (6)$$

will reject the signal coming from the interfering user having sequence $(\mathbf{X})^k$. This is true for any k , and by assigning the N cycle shifts of a single M -sequence to N subscribers, we have a network that can support N simultaneous users without any interference. Complete orthogonality between the users is achievable theoretically.

B. Hadamard Codes

A Hadamard Code is obtained by selecting as codes the rows of a Hadamard matrix. It is well known that an $(N \times N)$ Hadamard matrix of 1's and 0's has the property that any row differs from any other row in exactly $N/2$ positions. All rows except one contains $N/2$ zeros and $N/2$ ones. As an example, for $N = 4$

$$M_4 = \begin{pmatrix} 1 & 1 & 1 & 1 \\ 1 & 0 & 1 & 0 \\ 1 & 1 & 0 & 0 \\ 1 & 0 & 0 & 1 \end{pmatrix} \quad \bar{M}_4 = \begin{pmatrix} 0 & 0 & 0 & 0 \\ 0 & 1 & 0 & 1 \\ 0 & 0 & 1 & 1 \\ 0 & 1 & 1 & 0 \end{pmatrix}.$$

Taking (\mathbf{X}) as being row i and (\mathbf{Y}) as being row j with $i \neq j$, it is easy to verify that

$$\Theta_{\mathbf{X}\mathbf{Y}}(i, j) = \Theta_{\bar{\mathbf{X}}\mathbf{Y}}(i, j) \quad (7)$$

where $\bar{\mathbf{X}}$ is from \bar{M}_4 , therefore satisfying (4). In particular, we note that Hadamard codes allow orthogonal signaling in place of ASK. This is possible because for Hadamard codes we also have that

$$\Theta_{\mathbf{X}\bar{\mathbf{Y}}}(i, j) = \Theta_{\bar{\mathbf{X}}\bar{\mathbf{Y}}}(i, j).$$

This is simply not true for M -sequences. This allows gaining back a 3-dB loss inherent to the previously designed system. Finally, note that for an $N \times N$ Hadamard matrix, $N-1$ subscribers can be accommodated since the codeword containing all 1's has to be rejected.

C. Bipolar Codes

Any complex number can be represented as a combination of real, unipolar components. For practical reasons when designing the masks, we limit ourselves to $(-1, 1)$ codes. We recall that, one can represent a bipolar sequence $(\mathbf{Y}) = (y_0, y_1, \dots, y_{N-1})$ by its unipolar version $(\mathbf{Y}^u) = (y_0^u, y_1^u, \dots, y_{2N-1}^u)$. We note that

$$\begin{aligned} y_{2i}^u &= 1 & y_i &= 1 \\ &= 0 & y_i &= -1 \\ y_{2i+1}^u &= 0 & y_i &= 1 \\ &= 1 & y_i &= -1 \end{aligned} \quad (8)$$

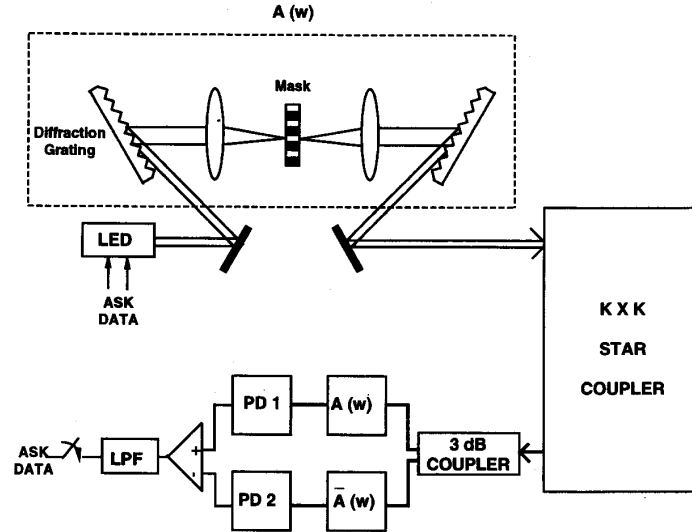


Fig. 2. Block diagram of a noncoherent FE-CDMA system.

Therefore, the condition $Z = \theta_{\mathbf{X}^u \mathbf{Y}^u}(k) - \theta_{\bar{\mathbf{X}}^u \mathbf{Y}^u}(k) = 0$ is equivalent to

$$\begin{aligned} Z &= 2 \left[\sum_{i=0}^{2N-1} x_i^u y_i^u \right] - \sum_{i=0}^{2N-1} y_i^u \\ &= 2 \left[\sum_{i=0}^{N-1} \frac{(x_i + 1)(y_i + 1)}{2} + \sum_{i=0}^{N-1} \frac{(1 - x_i)(1 - y_i)}{2} \right] \\ &\quad - \sum_{i=0}^{2N-1} y_i^u \\ &= \sum_{i=0}^{N-1} x_i y_i = \Theta_{\mathbf{X}\mathbf{Y}}(0) = 0. \end{aligned} \quad (9)$$

which is the usual bipolar crosscorrelation function. Therefore, all orthogonal ($\theta_{\mathbf{X}\mathbf{Y}}(0) = 0$) bipolar $(-1, 1)$ codes will satisfy (4) and can be applied to our system. For a unipolar sequence of length $2N$, only N subscribers however can be accommodated. This introduces no problem when the number of resolvable frequency slots is large enough. Namely, we look at sequences for which $(\mathbf{Y}) = (\mathbf{X})^k$

$$\Theta_{\mathbf{X}}(k) = \sum_{i=0}^{N-1} x_i x_{i+k} = 0 \quad \text{for all } k \neq 0$$

These sequences are termed Perfect Autocorrelation Sequences (PAS). However, it has been proven that no solution exists for $4 < N \leq 12100$. Almost (PAS) which have all out-of-phase autocorrelation values equal to 0 except 1 were recently proposed [14] and could be used for our system. For a bipolar sequence of length N , $2N$ frequency slots would be necessary and $N-1$ subscribers could be supported. Note that, for all unipolar sequences obtained from bipolar sequences, orthogonal signaling can be used. We have mentioned these sequences for completeness. In the following however, we will consider only m -sequences and Hadamard codes since they utilize the source spectrum more efficiently.

V. TRANSMITTER AND RECEIVER DESCRIPTION

Consider Fig. 2 which shows the transmitter and the receiver needed for a pair of communicating users. At the transmitter, the data directly modulates the optical source, which is then directed to the temporally nondispersive lens and grating apparatus presented before, for the spectral encoding operation. At the receiver, the following needs be realized: $\theta_{\bar{\mathbf{X}}\mathbf{Y}}(k) - \theta_{\mathbf{X}\mathbf{Y}}(k)$. This can easily be done by using 2 photodetectors, one to receive $\sum x_i x_{i+k}$ and the other to receive $\sum (1 - x_i) x_{i+k}$ and subtracting their outputs. One way of doing this, although probably not the most efficient, is to split the incoming signal in two parts, each one going through a separate lens and grating apparatus. Two masks that transmit complementary frequency bands are then needed. The notation $\bar{A}(w)$ in Fig. 2 simply means that the mask pattern in that branch is the opposite of the one used for $A(w)$. Another way which uses only one encoding apparatus, is to replace the spherical lenses by cylindrical lenses and to use a two-dimensional mask, where one dimension is still used for the frequency while the other is used to place the two complementary amplitude patterns. Of course, in a CDMA application, it is necessary that each user can communicate with every other user. Although the two masks at the receiver can be fixed, the one at the transmitter needs be programmable. This can be done, as already experimentally demonstrated, using Spatial-Light-Modulators based on Liquid-Crystal-Display (LCD) technology.

Note that, the desired signal is received only by photodetector 1, so that a 3 dB loss due to the coupler is inherent to the detector when using m -sequences. One way to efficiently use the balanced receiver for the transmitted data would be to use orthogonal signalling. When transmitting a "0", the spectrum is encoded by $A(w)$, while to transmit a "1", the spectrum is encoded by $\bar{A}(w)$. However, as we will discuss later, this would require at the transmitter, programmable masks with a

response time shorter than a bit period. For R_b in the Mbit/s range, this is still challenging with current technology.

Looking at the architecture of the proposed system, we see that it requires only low-cost broadband incoherent sources (compared to mode-locked sources) and simple direct detection receivers (no optical threshold element is needed). Furthermore, the spreading gain is independent of the bit rate since the coding in the frequency domain will not affect the signal in the time domain, significantly. This is a major advantage for a network that supports different kinds of services at different bit rates. The bandwidth of the receiver and the associated electronics need only match the bandwidth of the information signal, and not the chip rate.

VI. PRACTICAL CONSIDERATIONS

In this section, we address some practical concerns on the implementation and application of the proposed FE-CDMA system.

A. Spectral Shape of the Optical Sources

In the above discussion, it was implicitly assumed that all the 1's in the sequence will appear as 1's at the photodetector. However, the spectrum of a LED is not flat. It might exhibit for example a Gaussian shape, meaning that some 1's will be seen as different values depending on the position they take along the spectrum. The consequence of that will be a loss of perfect orthogonality among the users. There are basically three ways to counter this effect. The first is to use programmable Spatial Light Modulators (SLM), such as liquid crystal devices, in order to obtain nonbinary amplitude transmissions. Alternatively, one can assign different lengths of frequency bands depending on the chips positions in the codes, so that the power transmitted in each band will be the same. This however increases the complexity of mask fabrication. The second one is to equalize the LED spectrum, up to some degree, by using Acousto-Optical Tunable Filters, in the same way they have been used in optical systems with optical amplifiers [15]. Finally, one can simply reduce the length of the total frequency band that is encoded to be in the center of spectrum, which is flatter. In this paper, we concentrate on this solution. To see the effect of the spectral shape of the source, we have calculated the Signal-to-Interference Ratio (SIR) for different possibilities. We assume the code used is an M -sequence of length $N = 127$, a different cycle-shift of the same sequence is assigned to each subscriber. The SIR can be written as

$$\text{SIR} = \frac{(\sum_{i=0}^{N-1} x_i z_i)^2}{\sum_{k=1}^K (\sum_{i=0}^{N-1} x_i x_{i+k} z_i - \sum_{i=0}^{N-1} (1-x_i) x_{i+k} z_i)^2} \quad (10)$$

where z_i depends on the spectral shape of the source. We consider three cases:

1) Gaussian shape

$$z_i = \frac{1}{(2\pi\sigma^2)^{1/2}} \int_{(-B/2\alpha+iB/N\alpha)}^{(-B/2\alpha+(i+1)B/N\alpha)} e^{-f^2/2\sigma^2} df \quad (11)$$

where B is the 3-dB bandwidth of the source ($B = 2.354\sigma$), α is a design parameter related to the encoded bandwidth and $\alpha = 1$ when we encode the 3-dB bandwidth of the source. As α is increased the encoded bandwidth is reduced and the code looks more binary at the receiver.

2) Cosinusoidal shape

$$z_i = \int_{-B/2}^{B/2} X + \frac{X}{A_m} \cos\left(\frac{2\pi T f}{B}\right) df \quad (12)$$

where X represents the mean spectral height.

This shape is chosen to see the effect of ripples of different amplitudes A_m and different period T , on the SIR. It might correspond also to an unperfectly equalized spectrum.

3) Sinusoidal shape

$$z_i = \int_{-B/2}^{B/2} X + \frac{X}{A_m} \sin\left(\frac{2\pi T f}{B}\right) df. \quad (13)$$

In this case, the spectrum is asymmetric around the carrier frequency, and as it will be seen, the SIR is different from the cosinusoidal shape.

The results are shown on Fig. 3 and Fig. 4. On Fig. 3, the SIR (in dB) is plotted as a function of the number of active users for the three spectral shapes considered. Remember that for a perfectly flat spectrum the SIR would be infinite. The first observation is that the cosinusoidal and Gaussian spectra lead approximately to the same SIR, when $A_m = 4$, although they are very different shapes. The sinusoidal shape leads to a worse performance which might be an indication that an asymmetry around the carrier frequency is detrimental. As the period T of the cosinusoidal or sinusoidal shapes is changed from $T = 1$ to $T = 9$, the effect on the SIR is minor. However, as the amplitudes of the ripples is reduced, the SIR increases by more than 5 dB, for 40 users and a cosinusoidal shape. Note that, the value $A_m = 2$ corresponds to a very badly equalized spectrum since the amplitude of the ripples is the same as the mean value X . On Fig. 4, the SIR is plotted as a function of α , for 20, 60 and 100 active users, and for a Gaussian spectrum. As expected, increasing α leads to a higher SIR since the spectrum looks flatter. However, the power received would be smaller, since the encoded spectrum is reduced. This effect is not seen here, but will be observed in the next section when we calculate the bit error probability.

B. Programmable Amplitude Masks

In a CDMA network, it will usually be required that each user should be able to communicate with all other subscribers. In the context of a FE-CDMA system this implies that the mask used to code the spectrum of the source at the transmitter should be programmable. Alternatively, the masks at the receiver could be made programmable. However, it is more convenient to make the mask at the transmitter programmable since there is only one mask, compared to two at the receiver. Programmable Spatial Light Modulators (SLM), electrically addressed or optically addressed, are useful in many applications in optics so that they have been available for a long time. Probably the most commonly used type of

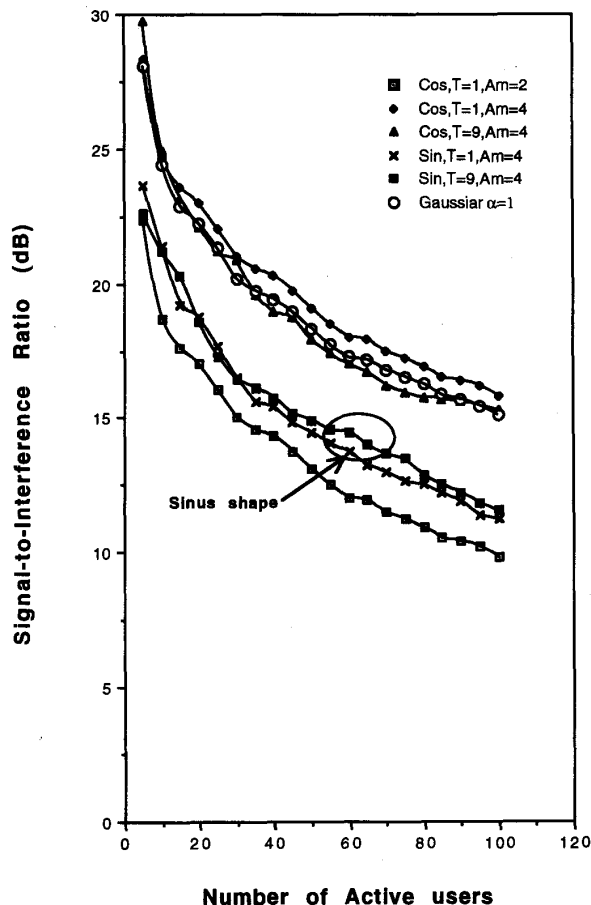


Fig. 3. SIR versus number of active users for different spectral shapes.

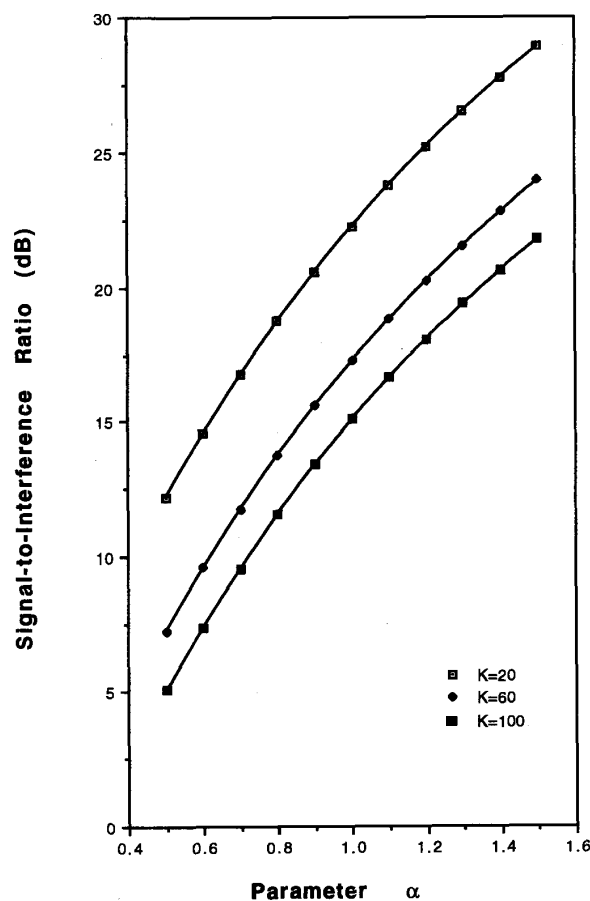


Fig. 4. Effect of the encoded bandwidth on the SIR for a gaussian spectral shape.

electrically addressed SLM is the Liquid Crystal Television (LCTV) panel, as it offers simplicity and a low-cost. However, recent applications such as pulse shaping by spectral phase modulation [16] and by spectral amplitude modulation [17] require lower losses and higher speeds, so they lead to the development of specially designed liquid crystal modulator array. One can find a summary of the state-of-the-art for smart-pixels, SLM based on liquid crystal technology in [18].

In our application, as well as in the case of coherent FE-CDMA, the main SLM parameters of interest are its speed and its optical contrast ratio, defined as the ratio of output optical power for a pixel being in the ON state to that of a pixel in the OFF state. For current commercially available devices, this ratio is usually larger than 100.

Qualitatively, a finite contrast ratio will reduce the desired signal power at the receiver since the power of the OFF pixels at the transmitter will flow through the lower branch of the receiver. In the upper branch nothing is changed, since the masks used at the receiver are fixed plates (transparencies or others), having an infinite contrast ratio.

For an interfering signal, the effect will be minimal if approximately half of the power in the OFF pixels of the interfering code goes through the upper branch and half goes

through the lower branch. This will be indeed the case when using Hadamard codes, but not quite when using M -sequences (the number of 0's is odd in this case). If the spectrum is flat, it is easy to see that a finite contrast ratio would have little effect on the multiple-access capacity of the system. In the next section, we will show the quantitative effects when one is using an M -sequence of period $N = 127$, and for a low contrast ratio value of 10.

The other major concern is the switching time required for a pixel to go from one state to another. One future application of the FE-CDMA system designed in the paper is its use as a routing technique for ultra fast Asynchronous Transfer Mode (ATM) switches. We will discuss this application in Section VIII. For an ATM switch, a packet has a fixed length of 53 bytes and is called a cell. Assuming a bit rate of 500 Mbt/s, a cell is transmitted in $0.85 \mu s$, so that the time to program a new address on the SLM should be a fraction of that value. For present SLM's, this is still challenging, although rapid progress is being made [19]–[20]. However, one should remember that SLM's are two-dimensional devices, having usually between 200 and 300 rows, most of them being independently programmable. Encoding the spectrum requires only one row. A possible solution to the speed limit, for a

switch application, could be to program the other unused rows in advance, by reading the address of the packets waiting in the queue. An LED array whose elements are associated with different rows of the SLM could be used, as done in the context of a free-space optical interconnect.

C. Dispersion

It is interesting to note that in the context of LAN's or switches, the orthogonality of the codes tolerates dispersion. That is, locally, as long as the optical source spectrum is flat, the codes will remain orthogonal. Suppose one is to use such a technique over a wide area network as a mean of multiplexing. It is clear that in any LED system, dispersion will limit the system length (10 s of kilometers at most) due to intersymbol interference of adjacent data bits. However, the resulting degradation would not be more severe than that due to a nonflat spectrum. We have already demonstrated that even with a nonflat spectrum, a substantial number of active users can be supported. Therefore overall, this multi-access method offers a good deal of tolerance to dispersion, even over longer distances.

VII. PERFORMANCE EVALUATION

In this Section, we will evaluate the bit error probability taking into account the Multi-Access Interference (MAI), the shot noise and the thermal noise. Since for EE-LED's or SLD's the transmitted power can be limited, we will not just plot the Bit Error Rate (BER) floors. We will rather seek the number of required photons/bit for a given value of P_e , as a function of the number of active users.

As in our work in [21], the entire system is linear in power, and the Moment Generating Function (MGF) can be easily found. We will therefore use the saddle point approximation to calculate the average probability of error. However, as it will be shown, the Gaussian approximation gives results almost identical (it gives a tight upper bound) to those observed by using the saddlepoint technique. The Gaussian approximation is used for most of the presented results. The results will be presented assuming the spectral shape is Gaussian. Following the expressions in [21], the MGF of the decision variable z is simply

$$M_z(s) = \prod_k M^k(s) e^{\lambda^0 (e^s - 1)} e^{\sigma^2 s^2 / 2}. \quad (14)$$

For our calculations, we choose $T^\circ = 293$, $R = 100$ and $1/T = 500$ Mbt/s. The MGF for one interfering signal is easily expressed as

$$M^k(s) = \sum_{I_1^k, I_0^k} \frac{1}{T} \int_0^T e^{(c1+c2\tau)(e^s-1)} e^{(c3+c4\tau)(e^{-s}-1)} d\tau \quad (15)$$

where

$$\begin{aligned} c1 &= \lambda_1^k I_0^k T \\ c2 &= \lambda_1^k [I_1^k - I_0^k] \\ c3 &= \lambda_2^k I_0^k T \\ c4 &= \lambda_2^k [I_1^k - I_0^k] \end{aligned}$$

We will consider only Amplitude Shift Keying (ASK) modulation and therefore $b_0, I_1^k, I_0^k \in \{0, 1\}$. The delay τ is uniform over the bit period. The factors λ_1^k and λ_2^k are the mean intensities received on the positively and negatively biased photodetectors respectively, for the interfering user k . Their expressions, and the expression for λ^0 are

$$\lambda_1^k = \frac{\eta PT}{hf} \sum_{i=0}^{N-1} x_i x_{i+k} z_i \quad (16)$$

$$\lambda_2^k = \frac{\eta PT}{hf} \sum_{i=0}^{N-1} (1 - x_i) x_{i+k} z_i \quad (17)$$

$$\lambda^0 = \frac{\eta PT}{hf} \sum_{i=0}^{N-1} x_i z_i \quad (18)$$

where variable z_i was defined in (11).

When using the Gaussian approximation, it is sufficient to find the mean and the variance of the decision variable z . They are easily found to be

$$\eta_z = \lambda^0 b_0 + \frac{1}{2} \sum_{k=1}^K (\lambda_1^k - \lambda_2^k) \quad (19)$$

$$\begin{aligned} \sigma_z^2 &= \lambda^0 b_0 + \frac{1}{2} \sum_{k=1}^K (\lambda_1^k + \lambda_2^k) \\ &+ \frac{1}{4} \sum_{k=1}^K (\lambda_1^k - \lambda_2^k)^2 + \sigma_{th}^2 \end{aligned} \quad (20)$$

Note that, the second term in (20) comes from the fact that the shot noise processes produced by the two photodetectors are independent, while the third term would be zero in the case of perfect cancellation of the interfering signals. As it can be seen, this would occur for a flat spectral density ($z_i = cte$). The factor 1/4 in front of the third term in (20) is true if we assume that all users are bit synchronized, ($\tau_k = 0$) for all k . For a uniform τ_k over $[0, T]$ it would be 1/6. The reason for assuming bit synchronized users is for the ATM switching application discussed in Section VIII. In this case, the packets at the input ports will be routed to their destination output ports at the same time, so that there is no random delay among them.

VIII. FE-CDMA SYSTEMS FOR ULTRAFAST ATM SWITCHING

Before presenting the results obtained from the performance calculations, we will briefly discuss one application of our system: routing in packet switches. The Asynchronous Transfer Mode (ATM) is a promising technique for switching different kinds of services in future broadband ISDN (B-ISDN). The required switch capacity depends strongly on the application and can range from several Gbt/s in small Local Area Networks, to a few Tb/s in B-ISDN exchange offices. As an example, if 100 000 customers are served each with a STS-3c line (155.52 Mbt/s), a capacity of 1.5 Tb/s will be needed for a ten percent traffic load [22].

Electronic ATM switches have been extensively developed but their throughput is limited by the operation speed limit of LSI's and signal transmission bandwidth limit. It is expected that the bottleneck of large capacity switching systems

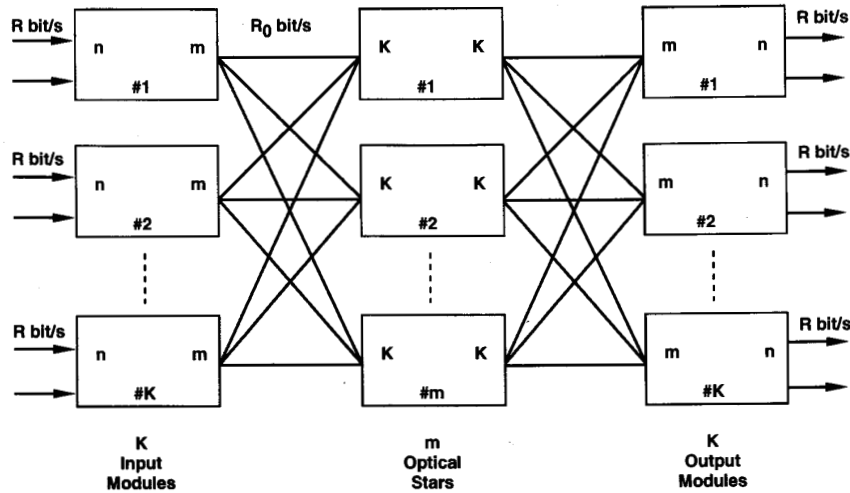


Fig. 5. A growable ATM switch architecture.

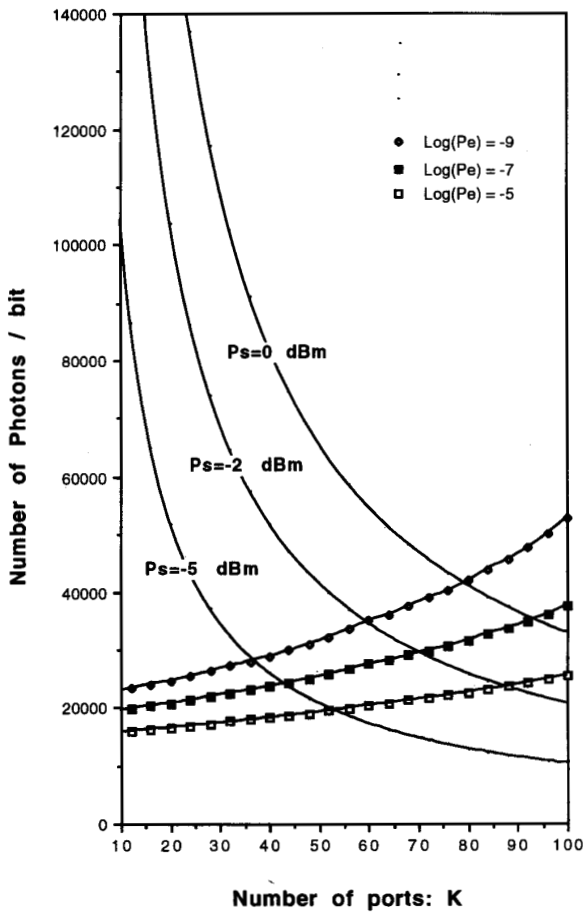


Fig. 6. Number of photons needed for a fixed P_e , $N = 127$ M -sequences, p-i-n photodetectors.

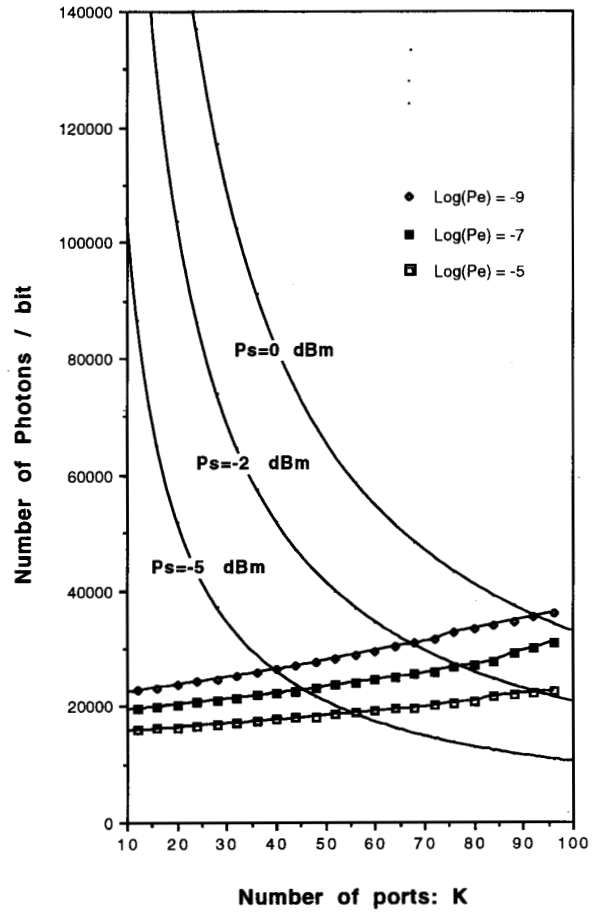


Fig. 7. Number of photons needed for a fixed P_e , $N = 128$, Hadamard codes, p-i-n photodetectors.

made up of electronic components will arise first in the interconnection of modules or boards. Optical interconnects with self-routing ability may be an efficient solution to this problem [22]. Switch architectures that combine the strength

of electronics for contention resolution and buffering and the strength of optics for routing and signal transmission are therefore suitable. Optical routing strategies include those based on wavelength [22-23] and time domain multiplexing

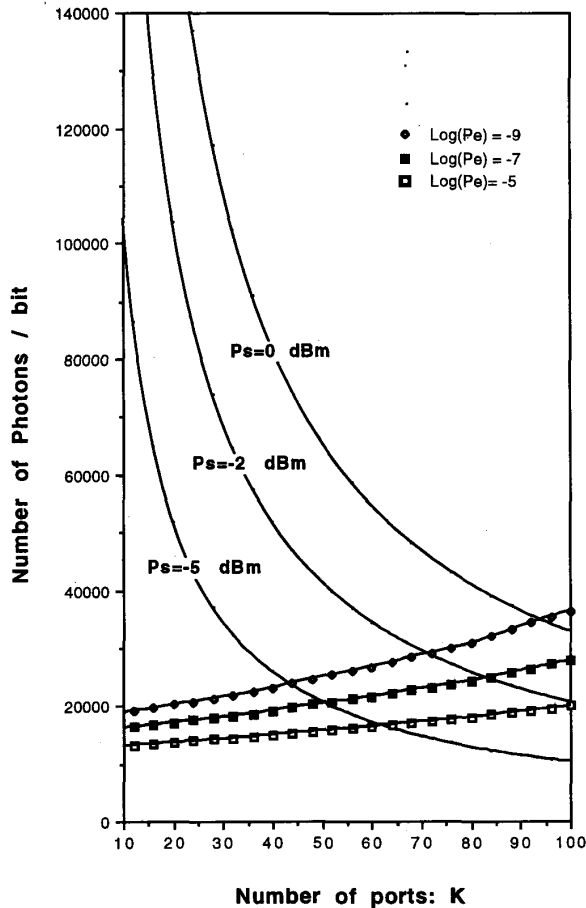


Fig. 8. Number of photons needed for a fixed P_e , $N = 511$ M -sequences, p-i-n photodetectors.

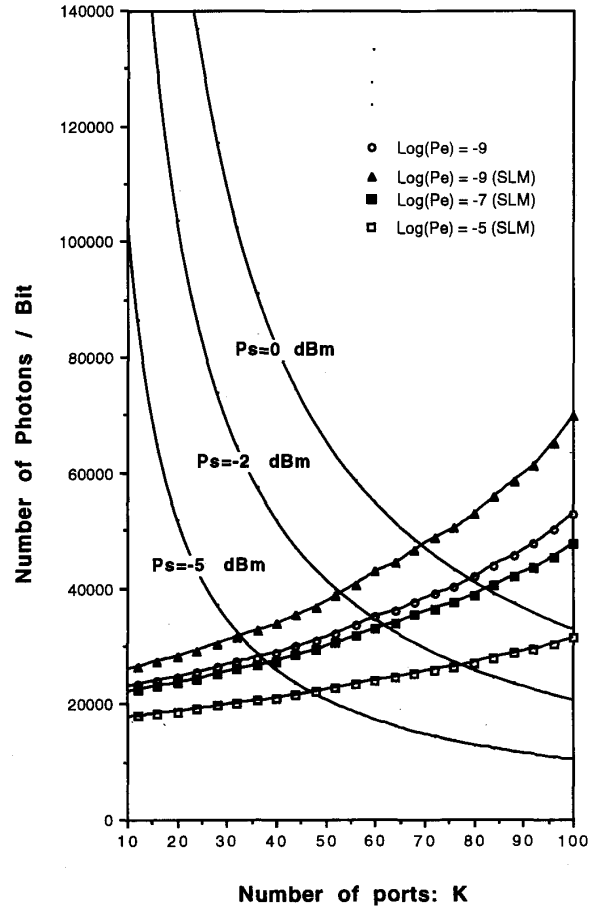


Fig. 9. Number of photons needed for a fixed P_e , $N = 127$ M -sequences, contrast ratio = 10 dB.

[24], as well as CDMA. A new optical routing strategy can be obtained from the incoherent FE-CDMA just discussed. Our routing technique can be used in many packet switch architectures, among them are the ones described in [22] and more recently in [25]. They both take the form shown in Fig. 5. In [25], m is larger than n and the structure generalizes the knockout principle to a group of n outputs. Buffering is only done at the output. In [22], $n > m$ and the structure uses shared input and output buffers based on memory chips developed by Hitachi [26]. Following is a list of the involved parameters:

- 1) $L = nK$ input and output lines;
- 2) K input and output modules;
- 3) m optical stars, each with K input and output ports;
- 4) m transmitters (receivers), e.g., number of LED's in a LED array, for each of the K input (output) modules;
- 5) R : bit rate used in the input lines;
- 6) R_0 : bit rate for the optical signals in the optical interconnect ($R \times n = R_0 \times m$);

For $n > m$, a Contention Resolution Device (CRD) is needed to resolve output contention. Its role is to choose one cell for each output module for each of the m optical stars. Detailed description of the CRD can be found in [22]. When

the CRD is m times faster than the cell transmission time through one star, the m optical stars are busy at all times. Only up to m cells can be routed to the same output module in one cell transmission time and therefore there is a Head of the Line Blocking (HOL) probability. This probability can be reduced by increasing m . However, for K fixed, m is limited by the speed limit of the CRD. On the other hand, K is limited by the power divisioning occurring at the star couplers. The number of photons/bit (Ph) available at a receiver is given by

$$\text{Ph} = \frac{10^{(P_s - 10 \log K - 6)/10}}{R_0 h f} \quad (21)$$

where P_s is the source power in dB, $10 \log K$ is the splitting loss due to the star coupler, a total of 6 dB of other losses and R_0 is the bit rate. This will be plotted on the figures of the P_e shown in the next section, for P_s values of 0 dBm, -2 dBm and -5 dBm. The crossing points of Ph with the P_e curves determine the maximum value of K that can be used.

IX. RESULTS AND DISCUSSION

The results obtained are given on Figs. 6 to 11. Unless otherwise specified, these results assume a Gaussian shape,

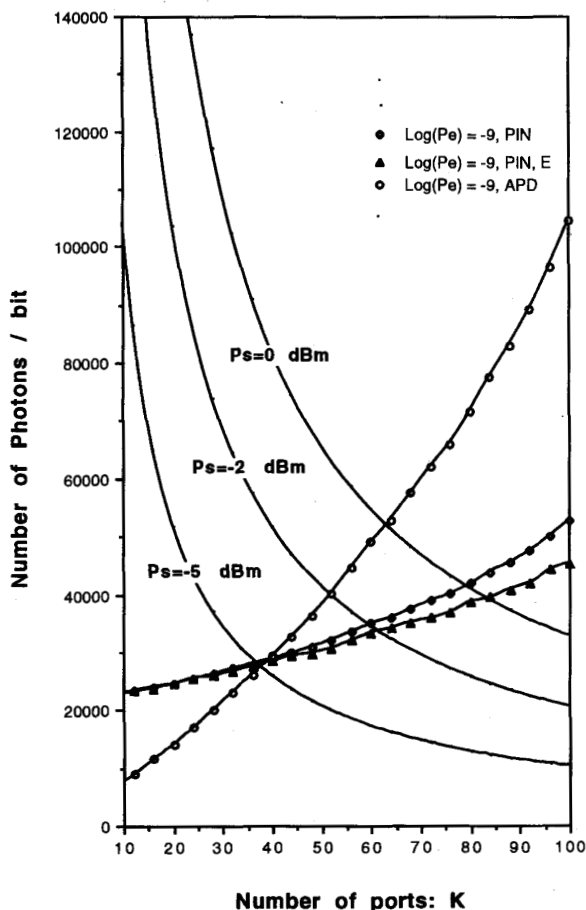


Fig. 10. Number of photons needed for $\text{Log}(P_e) = -9$, $N = 127$ M -sequences.

with $\alpha = 1.3$. The number of photons/bit required to get $P_e = 10^{-9}$, 10^{-7} and 10^{-5} is given, as well as the number of photons/bit available, for three power source values, from (21). The reason for considering different P_e values is that $P_e = 10^{-5}$ might lead to an acceptable probability of packet error. Unless otherwise stated, the results are calculated using the Gaussian approximation on the decision variable. The first matter to note is the number of active users (K). More than one hundred users can be accommodated for $P_e = 10^{-9}$. Note on Fig. 6 that, up to 70 interfering users, the power penalty is less than 3 dB. However, if the incoherent optical source can launch less than -2 dBm power, the multiple-access capacity will be limited to about 40. This is for a very reasonable code length of 127, for which a high-speed programmable SLM has already been developed for pulse shaping. On Fig. 7, Hadamard codes are considered instead of M -sequences. As seen, a better performance is obtained. Less than 3 dB penalty is observed for up to 100 users. The better performance can probably be explained by the fact that for a Hadamard code, the distribution of the ones and zeros across the spectrum is more uniform than for an M -sequence of length $N = 2^r - 1$, which always counts a run

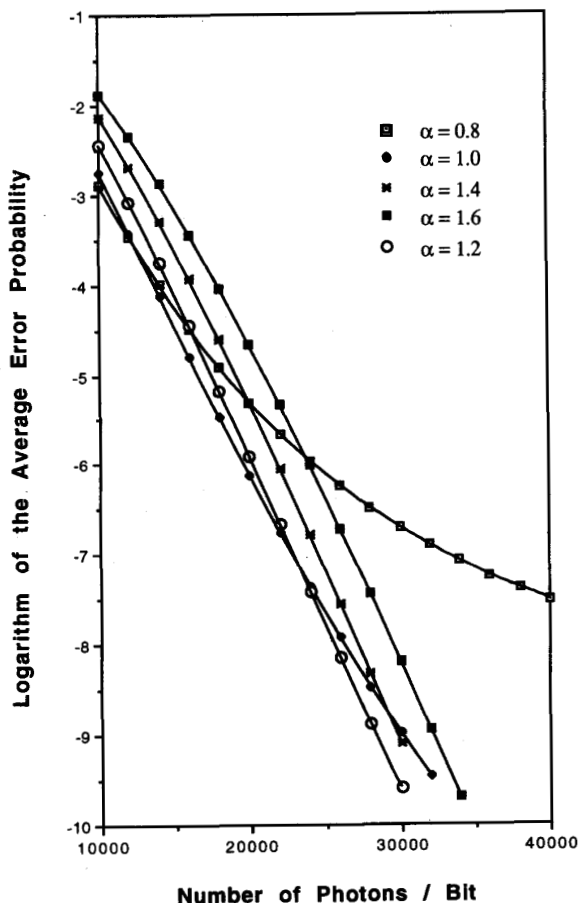


Fig. 11. Performance as the encoded bandwidth varies; $N = 127$ M -sequences, $K = 40$.

of r ones and $r - 1$ zeros. On Fig. 8, we show the effect of increasing the code length N to 511. A code length $N = 127$ is sufficient to accommodate 127 subscribers. However, by increasing the code length, the spectral length allocated to each chip is smaller, and the allocated power is therefore more uniform. As seen, the performance is better than with $N = 127$, but the requirement on the resolution of the spectral filtering is more severe. Tolerance to misalignments would also be greatly reduced.

In Fig. 9 we show the effect of having a finite contrast ratio (labeled SLM), taken to be 10 dB. As seen, 70 000 photons/bit are needed for $K = 100$, and $P_e = 10^{-9}$, compared to 54 000 photons/bit needed when the contrast ratio is 0. For other values of P_e there is little difference between a finite value, and an infinite value of the contrast ratio. We therefore believe that a finite contrast ratio from a programmable SLM would not be too harmful to our system. On Fig. 10, we compare the P_e obtained when using the saddlepoint approximation and the Gaussian approximation. As seen, the results of Gaussian approximation are very close to the "exact" results (curve labeled E). This yields a tight upper bound on the system performance. We also present the performance obtained when

using an APD with a gain G and an ionization coefficient $k = 0.1$. In this case, the expressions for the mean and variance need to be modified

$$\eta_z = G \left[\lambda_0 b_0 + \frac{1}{2} \sum_{k=1}^K (\lambda_1^k - \lambda_2^k) \right] \quad (22)$$

$$\sigma_z^2 = G^3 (1 - a^2 b) \left[\lambda_0 b_0 + \frac{1}{2} \sum_{k=1}^K (\lambda_1^k + \lambda_2^k) \right] + G^2 \left[\frac{1}{4} \sum_{k=1}^K (\lambda_1^k - \lambda_2^k)^2 \right] + \sigma_{th}^2. \quad (23)$$

An APD with the parameters considered would perform better only when the thermal noise dominates, which seems true for $K \leq 40$. When there are more active users, the shot noise dominates and a p-i-n is the right choice. It is interesting to see that the Gaussian and the saddlepoint approximations give identical results in the range where the thermal noise dominates. Finally, on Fig. 11 we plot the P_e as a function of the number of photons/bit for different values of the parameter α , and for $K = 40$ active users. It was observed in Fig. 4 that reducing the encoded bandwidth (increasing α) yields a higher SIR. One can see that taking into account the shot noise and the thermal noise, the highest α is not the best choice, since reducing the encoded bandwidth will reduce the received power, and therefore the Signal-to-Noise Ratio (SNR). Note that, for $\alpha = 0.8$, a floor is observed. In that case, the encoded bandwidth is too large and the spectrum is not flat enough, therefore, multiple-access-interference dominates and the P_e cannot be reduced by increasing the power.

Let us now estimate a possible achievable throughput for an ATM switch based on our encoding technique. Let us suppose $R_0 = 500$ Mbit/s as achievable by EE-LED's. For M -sequences with $N = 511$ in Fig. 8, the cell transmission time is $0.848 \mu\text{s}$ ($53 \text{ bytes} \times 8/R_0$). An arbitration cycle must therefore be over $0.848 \mu\text{s}$. A device that can achieve this in less than 22 ns is described in [22]. Taking a conservative value of 22 ns , we get $m \leq 42$. The total throughput T_R of the switch is given by

$$T_R = R_0 \times K \times m. \quad (24)$$

Assuming $P_e = 10^{-9}$ is needed and a value of $P_s = -2 \text{ dBm}$, K is limited to 72, from Fig. 8, and the achievable throughput is $T_R = 500 \text{ Mbit/s} \times 42 \times 72 = 1.5 \text{ Tb/s}$. To reduce the number of transmitters and receivers needed per module, we might choose $m = 10$ and the throughput decreases to $T_R = 360 \text{ Gbit/s}$. For $m = 20$, and assuming a $P_e = 10^{-7}$ is sufficient, one gets $T_R = 840 \text{ Gbit/s}$.

X. CONCLUSION

In this paper, we have presented a new type of CDMA system based on frequency encoding of optical broadband sources. Parts of this paper had been published by the same authors in [2]–[3]. We presented in detail a new design that applies to incoherent (broad-linewidth) sources. The proposed system has the advantage of using inexpensive optical sources,

and simple direct detection receivers with bandwidth requirements equal to the bit rate. The spreading gain of this type of CDMA system is independent of the bit rate since the spectral shaping of the sources does not affect the signals in the time domain. It was shown that a large number (from 70 to 100) active users can be supported, for a moderate code length of $N = 127$, with an operating average bit error rate of $P_e = 10^{-9}$. Application of such a system as a core module in an ATM switch was also briefly discussed.

REFERENCES

- [1] A. M. Weiner, J. P. Heritage, and J. A. Salehi, "Encoding and decoding of femtosecond pulses," *Opt. Lett.*, vol. 13, p. 300, 1988.
- [2] D. Zaccarin and M. Kavehrad, "An optical CDMA system based on spectral encoding of LED," *IEEE Photon. Technol. Lett.*, Apr. 1993.
- [3] D. Zaccarin and M. Kavehrad, "Ultrafast ATM switching using optical CDMA based on spectral encoding of LED," in *Proc. ICC*, New Orleans, May 1994.
- [4] A. M. Weiner *et al.*, "High-resolution femtosecond pulse shaping," *J. Opt. Soc. Am. B.*, vol. 5, pp. 1563–1572, Aug. 1988.
- [5] M. B. Danailov and I. P. Christov, "Time-space shaping of light pulses by fourier optical processing," *J. Mod. Optics*, vol. 36, pp. 725–731, 1989.
- [6] T. E. Chapuran, S. S. Wagner, and T. P. Lee, "Wavelength-dependent power penalties in broad band spectrally sliced WDM networks," in *Proc. OFC '92*, Paper TuN4, 1992.
- [7] G. D. Collins, "Achromatic fourier transform holography," *Appl. Optics*, vol. 20, pp. 3109–3119, Sept. 1981.
- [8] P. Anders, J. Lancis and W. D. Furlan, "White-light transformer with low chromatic aberration," *Appl. Optics*, vol. 31, pp. 4682–4687, Aug. 1992.
- [9] P. Cielo and C. Delisle, "Transmission d'images par modulation du spectre," *Can. J. Phys.*, vol. 54, pp. 2332–2339, 1976.
- [10] A. Lacourt and P. Boni, "Transmission d'images et d'hologrammes par une nappe de fibres optiques au moyen d'un codage chromatique," *Optics Commun.*, vol. 27, pp. 57–60, Oct. 1978.
- [11] T. Ohtuka *et al.*, "Single-mode fiber transmission using edge-emitting LED for broadband subscriber loops," *Electron. Commun. Japan*, part 1, vol. 72, May 1989.
- [12] Y. Kashima *et al.*, "Performance and reliability of InGaAsP superluminescent diode," *J. Lightwave Technol.*, vol. 11, pp. 1644–1649, Nov. 1992.
- [13] P. Wysocki *et al.*, "Spectral characteristics of high-power $1.5 \mu\text{m}$ broadband superluminescent fiber sources," *IEEE Photon. Technol. Lett.*, vol. 2, pp. 178–180, Mar. 1990.
- [14] J. Wolfmann, "Almost perfect autocorrelation sequences," *IEEE Trans. Inform. Theory*, vol. 38, pp. 1412–1418, 1992.
- [15] S. F. Su *et al.*, "Gain equalization in multiwavelength lightwave systems using aoustoopic tunable filters," *IEEE Photon. Technol. Lett.*, vol. 4, pp. 269–271, Mar. 1992.
- [16] A. M. Weiner *et al.*, "Programmable Shaping of femtosecond optical pulses by use of 128-element liquid crystal phase modulator," *J. Quantum Electron.*, vol. 28, pp. 908–920, 1992.
- [17] M. C. Wefers and K. A. Nelson, "Programmable phase and amplitude femtosecond pulse shaping," *Opt. Lett.*, vol. 18, pp. 2032–2034, 1993.
- [18] K. M. Johnson, D. J. McKnight, and I. Underwood, "Smart spatial light modulators using liquid crystals on silicon," *J. Quantum Electron.*, vol. 29, pp. 699–714, Feb. 1993.
- [19] G. Andersson *et al.*, "Submicrosecond electro-optic switching in the liquid-crystal smectic A phase: The soft-mode ferroelectric effect," *Appl. Phys. Lett.*, vol. 51, pp. 640–642, 1987.
- [20] J. Gourlay, P. McOwan, and D. G. Vass, "Time-multiplexed optical hadamard image transform with ferroelectric-liquid-crystal-over-silicon spatial light modulators," vol. 18, pp. 1745–1747, Oct. 1993.
- [21] D. Zaccarin and M. Kavehrad, "Performance evaluation of optical CDMA systems using noncoherent detection and bipolar codes," *J. Lightwave Technol.*, vol. 12, no. 1, Jan. 1994.
- [22] A. Cisneros and C. A. Brackett, "A large ATM switch based on memory switches and optical star couplers," *IEEE J. Select Areas Commun.*, vol. 9, pp. 1348–1360, Oct. 1991.
- [23] N. Shimosaka *et al.*, "Wavelength-addressed optical network using an ATM cell-based access scheme," in *Dig. OFC*, San Jose, Feb. 1993, Paper TuJ6, p. 49.

- [24] A. Jajszczyk and H. T. Mouftah, "Photonic fast ATM switching," *IEEE Commun. Mag.*, vol. 31, pp. 58-65, Feb. 1993.
- [25] K. Y. Eng., M. J. Karol, and Y. S. Yeh, "A growable packet (ATM) switch architecture: Design principles and applications," *IEEE Trans. Commun.*, vol. 40, pp. 423-430, Feb. 1992.
- [26] H. Kuwahara *et al.*, "A shared buffer memory switch for an ATM exchange," in *Proc. ICC*, June 1989, pp. 4.4.1-4.4.5.



Mohsen Kavehrad (S'75-S'75-M'78-SM'86-F'92) was born in Tehran, Iran, on January 1, 1951. He received his Ph.D. degree from Polytechnic University (Formerly: Brooklyn Polytechnic Institute), Brooklyn, NY, in November 1977 in Electrical Engineering.

Between 1978 and 1981, he worked for Fairchild Industries (Space Communications Group), GTE Satellite Corp. and GTE Laboratories in Waltham-Mass. In December 1981 he joined AT&T Bell Laboratories where he worked in Research,

Development, and Systems Engineering areas as a member of technical staff. In March 1989 he joined the Department of Electrical Engineering at University of Ottawa, as a full professor. He is the Leader of Photonic Networks and Systems Thrust and a Project Leader in the Telecommunications Research Institute of Ontario (TRIO). Also, he is a project leader in the Canadian Institute for Telecommunications Research (CITR). Presently, he is the Director of Ottawa-Carleton Communications Center for Research (OCCCR). In the summer of 1991, he was a visiting researcher at NTT Laboratories in Japan. He has worked in the fields of satellite communications, point-to-point microwave radio communications, portable and mobile radio communications, atmospheric laser communications, and optical fiber communications and networking. He has published over 150 papers and has several patents issued in these fields.

Dr Kavehrad is a former Technical Editor for the *IEEE TRANSACTIONS ON COMMUNICATIONS*, *IEEE COMMUNICATIONS MAGAZINE*, and the *IEEE MAGAZINE OF LIGHTWAVE TELECOMMUNICATIONS SYSTEMS*.

Denis Zaccarin was born in Québec city, Canada, on November 24, 1964. He received the B.Sc.A. and M.Sc. degrees in electrical engineering from Laval University, Québec, Canada, in 1987 and 1989, respectively, and the Ph.D. degree in electrical engineering from University of Ottawa in 1994.

In 1988 he served as Consultant for the Canadian government in the area of satellite communication systems. In 1989-1990, he worked as a research engineer for the Department of National Defense, Ottawa, where he was involved in secure communication systems. He is a member of scientific staff at Bell-Northern Research, Ottawa, where he works in the area of high-speed optical communication systems.